

ChemComm

Chemical Communications

Accepted Manuscript

This article can be cited before page numbers have been issued, to do this please use: C. Xing, J. Liu, F. Chen, Y. Li, C. Lv, Q. Peng, H. Hou and K. Li, *Chem. Commun.*, 2020, DOI: 10.1039/D0CC01031F.



This is an Accepted Manuscript, which has been through the Royal Society of Chemistry peer review process and has been accepted for publication.

Accepted Manuscripts are published online shortly after acceptance, before technical editing, formatting and proof reading. Using this free service, authors can make their results available to the community, in citable form, before we publish the edited article. We will replace this Accepted Manuscript with the edited and formatted Advance Article as soon as it is available.

You can find more information about Accepted Manuscripts in the [Information for Authors](#).

Please note that technical editing may introduce minor changes to the text and/or graphics, which may alter content. The journal's standard [Terms & Conditions](#) and the [Ethical guidelines](#) still apply. In no event shall the Royal Society of Chemistry be held responsible for any errors or omissions in this Accepted Manuscript or any consequences arising from the use of any information it contains.

COMMUNICATION

Diphenyl-1-pyrenylphosphine: Photo-triggered AIE/ACQ transition with remarkable third-order nonlinear optical signal changeReceived 00th January 20xx,
Accepted 00th January 20xxChang Xing,^{‡,a} Jianxun Liu,^{‡,a} Fang Chen,^a Yuanyuan Li,^{*b} Changjian Lv,^a Qiuchen Peng^{a,b}, Hongwei Hou,^{*a} and Kai Li^{*a}

DOI: 10.1039/x0xx00000x

A propeller-like pyrene derivative of diphenyl-1-pyrenylphosphine (DPPP) is designed and synthesized. DPPP exhibits unique photo-triggered AIE/ACQ transition with remarkable third-order nonlinear optical signal change, which is proved to be originated from the photo-induced oxidation of phosphorus atom.

Pyrene is a useful polycyclic aromatic hydrocarbon molecule which has four fused benzene rings with extensive π -electron delocalization. The abundant excited states of pyrene endow its derivatives with multiple photophysical properties such as photoluminescence, hole-transporting ability and nonlinear optical (NLO) properties, making it suitable for the applications of organic light-emitting diodes (OLEDs), organic field-effect transistors (OFETs), luminescence probes, NLO switches, etc.¹ However, the plane structure of pyrene usually leads to strong π - π interactions, which makes its fluorescence quench in concentrated solution or in solid state, *i.e.*, aggregation-induced quenching (ACQ) effect.² In order to inhibit π - π interactions, propeller-like structure was introduced to the design of pyrene derivatives, which endowed the compounds with intense emission in solid state due to the aggregation-induced emission (AIE) effect.³ Pyrene-based AIE molecules exhibited high quantum yield in solid state, which have been widely used in the development of OLEDs, OFETs, chemosensors, and bioimaging materials.⁴ However, there are few reports about pyrene-based AIE molecules with photo-responsive performance.

In this work, a propeller-like pyrene derivative of diphenyl-1-pyrenylphosphine (DPPP) was designed and synthesized, which exhibited expected AIE properties. Interestingly, DPPP showed unique photo-triggered AIE/ACQ transition with remarkable third-order NLO signal change, making it a promising material for photo-triggered luminescence switch and third-order NLO switch.

DPPP was synthesized according to the reported method (Scheme S1).⁵ The luminescence properties of DPPP in H₂O/EtOH mixtures with different water fractions (f_w) were studied firstly. As shown in Figure 1A, DPPP exhibited no visible emission when the water fraction (f_w) was lower than 50% but intense green emission when f_w was higher than 60%. Corresponding fluorescence spectra are shown in Figure 1B. There are three emission peaks (λ_{\max} = 379 nm, 399 nm and 419 nm) within the range of about 370 nm - 440 nm, which belong to I_I , I_{IV} and I_V characteristic emission peaks of pyrenyl, respectively.⁶ The fluorescence intensities of these three peaks enhanced gradually when f_w was lower than 80% and then started to decrease with increasing f_w . On the other hand, a new, broad emission peak (λ_{\max} = 507 nm) was observed when f_w was higher than 60% and the fluorescence intensity strengthened apparently by heightening f_w (Figure 1C).

These emission changes might be attributed to different existing forms of DPPP in different solvents. According to the reports, pyrene derivatives usually exhibit different emission properties in single molecule state, dimer state and aggregated state because of different π - π interactions and C-H \cdots π interactions.⁷ Thus, a mechanism for the emission change of DPPP was proposed and shown in Figure 1D. When f_w was 0% - 50%, DPPP was in single molecule state. There was no π - π interaction between the pyrenyl groups. As a result, free dynamic intramolecular rotations of the conjugate groups in DPPP happened, leading to an excited state non-radiative transition and fluorescence quenching. Thus, only weak purple emission belonging to pyrenyl moiety was detected, which was invisible by naked eyes. When f_w was 60% - 80%, the solubility of DPPP decreased and DPPP dimers formed. The π - π interactions between two pyrenyl groups enhanced the purple emission.⁸ Meanwhile, the intramolecular rotations of the conjugate groups were restricted effectively, resulting in an intense green emission of DPPP molecule. The origination of this green emission will be discussed later in this article. When f_w was higher than 90%, DPPP aggregations formed. The π - π interactions were replaced by C-H \cdots π interactions due to the steric-hindrance effect in aggregated state. As a result, the purple emission quenched, while the green emission was still intense because the intramolecular rotation was restricted.⁹

^a Green Catalysis Center, and College of Chemistry, Zhengzhou University, Henan 450001 (P. R. China), E-mail: likai@zzu.edu.cn

^b School of Chemistry and Chemical Engineering, Henan University of Technology, Henan, 450001 (P. R. China), E-mail: yuanyuanli@haut.edu.cn

[†] Electronic Supplementary Information (ESI) available: Details on experimental procedures. Additional experimental data, including crystal data, ¹H-NMR spectra, mass spectrometry, etc. CCDC: 1973777, 1973778. For ESI and crystallographic data in CIF or other electronic format see DOI: 10.1039/x0xx00000x

[‡] C. Xing and J. Liu contributed equally.

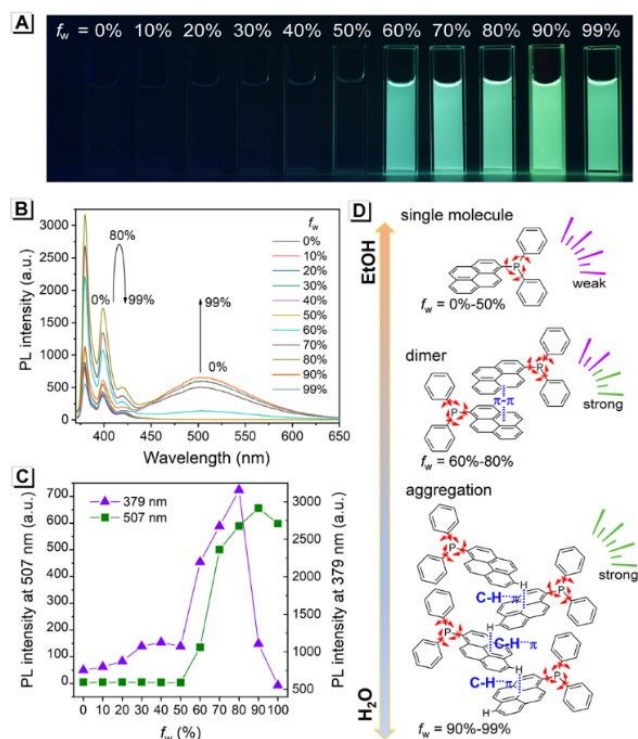


Figure 1. A) Photo and B) fluorescence spectra of **DPPP** in H₂O/EtOH mixtures with different f_w . C) Fluorescence intensity of **DPPP** as functions of f_w . The concentration of **DPPP** was 10 $\mu\text{mol}\cdot\text{L}^{-1}$. D) Proposed mechanism for the emission of **DPPP** in H₂O/EtOH mixtures with different f_w .

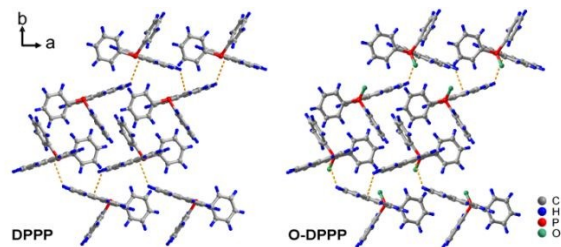


Figure 2. Crystal structure of **DPPP** and **O-DPPP**.

The packing form of **DPPP** in aggregated state was investigated by single-crystal X-ray diffraction (SCXRD) analysis. Single crystal of **DPPP** was grown from EtOH by slow solvent evaporation. As shown in Figure 2, **DPPP** exhibited a typical propeller-like structure. There was no π - π interaction but were a plenty of C-H... π interactions in the crystal of **DPPP**, which fitted well with the proposed mechanism shown in Figure 1D.

The mechanism was further supported by absorption spectra and dynamic light scattering (DLS) experiments. As shown in Figure S1, no level-off tail can be observed in the absorption spectra of **DPPP** in EtOH ($f_w = 0\%$). On the contrary, **DPPP** exhibited an obvious level-off tail in the absorption spectrum over 400 nm in water-dominated solvent ($f_w = 99\%$), which could be attributed to the light scattering of aggregated suspensions.¹⁰ Meanwhile, there were nano-particles with diameter around 242 nm in the solvent of $f_w = 99\%$ but no particles were observed in EtOH (Figure S2). These results

confirmed that **DPPP** was in dispersed state in EtOH but in an aggregated state in water-dominated solvent, respectively. Thus, we can conclude that the intense green emission of **DPPP** in water-dominated solvents was originated from its aggregations, *i.e.*, an AIE fluorescence. The α_{AIE} value of the green emission was 126.1, which was calculated using the ratio of I_{99}/I_0 , where I_{99} and I_0 are the emission intensities of **DPPP** at 507 nm in solution with $f_w = 99\%$ and 0%, respectively.¹¹ In the solvent of $f_w = 70\%$, **DPPP** exhibited no level-off tail in the absorption spectrum and no particles in DLS test, which was in accord with the characteristics of dimer.

Interestingly, after being irradiated by 365 nm UV light (power density = 12.8 mW/cm²) for 3 min, **DPPP** exhibited different photo-response performances in different solvents. **DPPP** turned from invisible purple fluorescence to intense blue fluorescence in EtOH (Figure 3A inset). On the contrary, the green emission of **DPPP** in water quenched after UV light irradiation (Figure 3B inset). Corresponding fluorescence spectra were recorded. As shown in Figure 3A and Figure 3B, the emission intensity of **DPPP** at 425 nm enhanced 11.4-fold after UV light irradiation in EtOH. In water, the emission peak at 507 nm disappeared while the emission intensities in the range of 370 nm - 425 nm increased. These phenomena suggested that **DPPP** turned from an AIE molecule to an ACQ molecule after UV light irradiation.

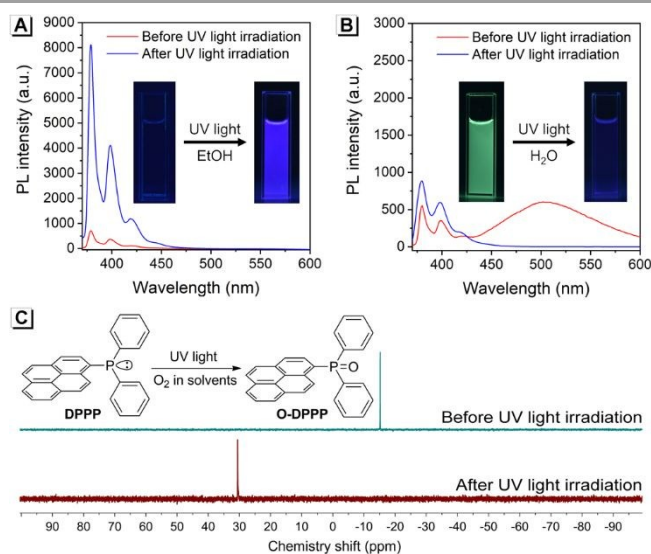


Figure 3. Photos and fluorescence spectra of **DPPP** in A) EtOH and B) H₂O before and after UV light irradiation. The concentration of **DPPP** was 10 $\mu\text{mol}\cdot\text{L}^{-1}$. C) ³¹P-NMR spectra of **DPPP** before and after UV light irradiation. Inset: Proposed mechanism for the photo-response process of **DPPP**.

To understand the mechanism of photo-response process of **DPPP**, ³¹P-NMR spectra of **DPPP** before and after UV light irradiation were investigated. As shown in Figure 3C, the chemical shift of phosphorus atom of **DPPP** turned from -15.18 to 30.58 after UV light irradiation, suggesting a formation of P=O group.¹² Thus, a mechanism for the photo-response process of **DPPP** was proposed (Figure 3C inset). As shown,

DPPP was oxidized upon UV light irradiation, producing an oxidized product of **O-DPPP**. The formation of **O-DPPP** was confirmed by high resolution mass spectrometry (HRMS) and $^1\text{H-NMR}$ spectra. As shown in Figure S3, a molecular ion peak of 403.1247 was found in the HRMS of **DPPP** after UV light irradiation, which agreed well with the theoretical value of **O-DPPP** ($[\text{M}+\text{H}]^+$ for **O-DPPP** was calculated as 403.1246). $^1\text{H-NMR}$ spectra showed that the chemical shifts of protons in UV light irradiated **DPPP** moved to lower field significantly (Figure S4). This result also certified the formation of **O-DPPP** because the strong electronegativity of oxygen in **O-DPPP** endows its protons with lower chemical shifts than that of **DPPP**. More importantly, all the peaks could be well assigned, demonstrating a high purity of **O-DPPP**.

To understand why **DPPP** turned from an AIE molecule to an ACQ molecule (**O-DPPP**) after UV light irradiation, crystal structures of **DPPP** and **O-DPPP** were compared. Surprisingly, the molecular geometries and crystal structures of **DPPP** and **O-DPPP** were highly similar (Figure 2 and Table S1), suggesting that the space effect was not an origination for their different emission properties in aggregated state. The fluorescence properties and existing states of **O-DPPP** in $\text{H}_2\text{O}/\text{EtOH}$ mixtures with different f_w were further studied. As shown in Figure 4A and Figure 4B, the emission intensities of **O-DPPP** in the range of 370 nm - 440 nm reached the maximum when f_w was 60%. Once f_w was beyond 60%, the fluorescence emission decreased rapidly. Meanwhile, DLS measurements suggested that there was no particle in the solutions with f_w below 60% but were nano-particles with diameter around 490 nm in the solvent of $f_w = 99\%$ (Figure S5). These results were analogous to that of **DPPP**, suggesting that **O-DPPP** had a similar emission mechanism to **DPPP**: When f_w was lower than 60%, the emission intensity of **O-DPPP** at 370 nm - 440 nm increased gradually because of the gradual formation of **O-DPPP** dimers with π - π interactions; When f_w was higher than 70%, nano-aggregations formed and the purple emission was quenched.

Interestingly, unlike **DPPP**, no green emission was observed for **O-DPPP** in all the mixed solvents. This result suggested that the green emission of **DPPP** might be closely related to the lone pair electrons in its phosphorus atom, which is the only difference between the structures of **DPPP** and **O-DPPP**. Thus, a possible mechanism for the green emission of **DPPP** was proposed. In aggregated state, the lone pair electrons can participate in the twisty conjugate system due to the immobilized conformation. The lone pair electrons connect two phenyl groups and one pyrenyl group, resulting in excimer emission with green emission. In dissolved state, the aromatic rings could rotate around the carbon-phosphorus single bonds, breaking the conjugation and quenching the green emission. This hypothesis was supported by density functional theory (DFT) calculations. As shown in Figure 4C, the highest occupied molecular orbital (HOMO) of **DPPP** is delocalized over the entire molecule, demonstrating the conjugation of the aromatic rings. On the contrary, the HOMO of **O-DPPP** is mostly covered on pyrenyl groups, suggesting that the aromatic rings are not conjugated. These differences are highlighted by red boxes in Figure 4C.

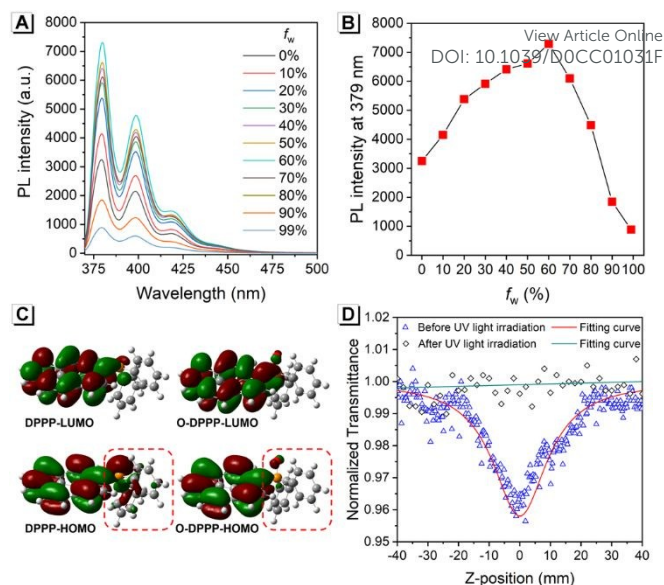


Figure 4. A) Fluorescence spectra of **O-DPPP** in $\text{H}_2\text{O}/\text{EtOH}$ mixtures with different f_w . B) Fluorescence intensity of **O-DPPP** at 379 nm as functions of f_w . The concentration of **O-DPPP** was $10 \mu\text{mol}\cdot\text{L}^{-1}$. C) The frontier molecular orbitals of **DPPP** and **O-DPPP** obtained *via* DFT calculations. D) Normalized Z-scan curve of **DPPP** before and after UV light irradiation.

Due to the existence of pyrene moiety, **DPPP** is expected to exhibit third-order NLO properties.¹³ Thus, Z-scan absorption spectrum of **DPPP** before and after UV light irradiation were recorded. As shown in Figure 4D, a normalized transmittance valley was observed in **DPPP** before UV light irradiation, suggesting a reverse saturation absorption (RSA) behaviour. After UV light irradiation, the third-order NLO signal of **DPPP** disappeared, which indicated that **O-DPPP** has no third-order NLO property. These results suggested that **DPPP** could be used as a photo-controlled switch not only with significant emission change, but also with remarkable third-order NLO signal change.

In summary, a propeller-like molecule of **DPPP** was designed and simply synthesized. Upon UV light irradiation, **DPPP** turned to **O-DPPP** completely. The fluorescence properties of **DPPP** and **O-DPPP** in different states were carefully studied, which indicated that **DPPP** is an AIE molecule while **O-DPPP** is an ACQ molecule. Moreover, a third-order NLO signal change of **DPPP** upon UV light irradiation was also observed. This unique photo-triggered AIE/ACQ transition of **DPPP** as well as remarkable third-order NLO signal change makes it a promising material for photo-triggered luminescence switch and third-order NLO switch.

This work was financially supported by the National Natural Science Foundation of China (No. U1904172, 21501150, 51502079, 21671174) and Zhongyuan thousand talents project.

Conflicts of interest

There are no conflicts to declare.

Notes and references

- (a) T. M. Figueira-Duarte and K. Müllen, *Chem. Rev.*, 2011, **111**, 7260-7314; (b) E. Cariati, C. Botta, S. G. Danelli, A. Forni, A. Giaretta, U. Giovannella, E. Lucenti, D. Marinotto, S. Righetto and R. Ugo, *Chem. Commun.*, 2014, **50**, 14225-14228; (c) L. Ascherl, E. W. Evans, J. Gorman, S. Orsborne, D. Bessinger, T. Bein, R. H. Friend and F. Auras, *J. Am. Chem. Soc.*, 2019, **141**, 15693-15699; (d) C. Fu, S. Luo, Z. Li, X. Ai, Z. Pang, C. Li, K. Chen, L. Zhou, F. Li, Y. Huang and Z. Lu, *Chem. Commun.*, 2019, **55**, 6317-6320; (e) J. Y. Shao, N. Yang, W. Guo, B. B. Cui, Q. Chen and Y. W. Zhong, *Chem. Commun.*, 2019, **55**, 13406-13409; (f) K. Takaishi, K. Iwachido and T. Ema, *J. Am. Chem. Soc.*, 2020, **142**, 1774-1779; (g) B. Wang, F. Zhang, S. Wang, R. Yang, C. Chen and W. Zhao, *Chem. Commun.*, 2020, DOI: 10.1039/c9cc07256j.
- (a) Z. Zhao, S. Chen, J. W. Y. Lam, P. Lu, Y. Zhong, K. S. Wong, H. S. Kwok and B. Z. Tang, *Chem. Commun.*, 2010, **46**, 2221-2223; (b) P. Alam, N. L. C. Leung, Y. Cheng, H. Zhang, J. Liu, W. Wu, R. T. K. Kwok, J. W. Y. Lam, H. H. Y. Sung, I. D. Williams and B. Z. Tang, *Angew. Chem. Int. Ed.*, 2019, **58**, 4536-4540.
- (a) J. Luo, Z. Xie, J. W. Y. Lam, L. Cheng, H. Chen, C. Qiu, H. S. Kwok, X. Zhan, Y. Liu, D. Zhu and B. Z. Tang, *Chem. Commun.*, 2001, 1740-1741; (b) J. Yang, L. Li, Y. Yu, Z. Ren, Q. Peng, S. Ye, Q. Li and Z. Li, *Mater. Chem. Front.*, 2017, **1**, 91-99; (c) X. Feng, C. Qi, H. T. Feng, Z. Zhao, H. H. Y. Sung, I. D. Williams, R. T. K. Kwok, Jacky W. Y. Lam, A. Qin and B. Z. Tang, *Chem. Sci.*, 2018, **9**, 5679-5687; (d) M. M. Islam, Z. Hu, Q. Wang, C. Redshaw and X. Feng, *Mater. Chem. Front.*, 2019, **3**, 762-781.
- (a) H. Lee, B. Kim, S. Kim, J. Kim, J. Lee, H. Shin, J.-H. Lee and J. Park, *J. Mater. Chem. C*, 2014, **2**, 4737-4747; (b) X. Gao and Z. Zhao, *Sci. China Chem*, 2015, **58**, 947-968; (c) X. Feng, J.-Y. Hu, C. Redshaw and T. Yamato, *Chem. Eur. J.*, 2016, **22**, 11898-11916; (d) K. Oniwa, H. Kikuchi, H. Shimotani, S. Ikeda, N. Asao, Y. Yamamoto, K. Tanigaki and T. Jin, *Chem. Commun.*, 2016, **52**, 4800-4803; (e) J. Yang, Q. Guo, X. Wen, X. Gao, Q. Peng, Q. Li, D. Ma and Z. Li, *J. Mater. Chem. C*, 2016, **4**, 8506-8513; (f) V. K. Singh, R. Prasad, B. Koch, S. H. Hasan and M. Dubey, *New J. Chem.*, 2017, **41**, 5114-5120; (g) C.-Z. Wang, Y. Noda, C. Wu, X. Feng, P. Venkatesan, H. Cong, M. R. J. Elsegood, T. G. Warwick, S. J. Teat, C. Redshaw and T. Yamato, *Asian J. Org. Chem.*, 2018, **7**, 444-450; (h) J. Yang, Z. Chi, W. Zhu, B. Z. Tang and Z. Li, *Sci. China Chem.*, 2019, **62**, 1090-1098; (i) X. Feng, Z. Xu, Z. Hu, C. Qi, D. Luo, X. Zhao, Z. Mu, C. Redshaw, J. W. Y. Lam, D. Ma and B. Z. Tang, *J. Mater. Chem. C*, 2019, **7**, 2283-2290; (j) X. Feng, J. Zhang, Z. Hu, Q. Wang, M. M. Islam, J.-S. Ni, M. R. J. Elsegood, J. W. Y. Lam, E. Zhou and B. Z. Tang, *J. Mater. Chem. C*, 2019, **7**, 6932-6940; (k) Q. Li and Z. Li, *Sci. China Mater.*, 2020, **63**, 177-184.
- R. F. Brissos, P. Clavero, A. Gallen, A. Grabulosa, L. A. Barrios, A. B. Caballero, L. Korrodi-Gregório, R. Pérez-Tomás, G. Muller, V. Soto-Cerrato and P. Gamez, *Inorg. Chem.*, 2018, **57**, 14786-14797.
- (a) M. E. Haque, S. Ray and A. Chakrabarti, *J. Fluoresc.*, 2000 **10**, 1-6; (b) M. I. Burguete, F. Galindo, E. García-Verdugo, N. Karbass and S. V. Luis, *Chem. Commun.*, 2007, 3086-3088.
- (a) A. Gulyani, N. Dey and S. Bhattacharya, *Chem. Commun.*, 2018, **54**, 5122-5125; (b) Y. Zhang, B. He, J. Liu, S. Hu, C. Pan, Z. Zhao and B. Z. Tang, *Phys. Chem. Chem. Phys.*, 2018, **20**, 9922-9929; (c) Q. Wang, Q. Zhang, Q. W. Zhang, X. Li, C. X. Zhao, T. Y. Xu, D. H. Qu and H. Tian, *Nat. Commun.*, 2020, **11**, 158.
- (a) D. S. Karuppannan and D. J. C. Chambron, *Chem. Asian J.*, 2011, **6**, 964-984; (b) Y. Wu, J. Wang, F. Zeng, S. Huang, J. Huang, H. Xie, C. Yu and S. Wu, *ACS Appl. Mater. Interfaces*, 2016, **8**, 1511-1519; (c) D. Niu, Y. Jiang, L. Ji, G. Ouyang and M. Liu, *Angew. Chem. Int. Ed.*, 2019, **58**, 5946-5950.
- (a) J. Mei, N. L. C. Leung, R. T. K. Kwok, J. W. Y. Lam and B. Z. Tang, *Chem. Rev.*, 2015, **115**, 11718-11940; (b) K. Li, Y. Liu, Y. Li, Q. Feng, H. Hou and B. Z. Tang, *Chem. Sci.*, 2017, **8**, 7258-7267; (c) J. Liu, C. Xing, D. Wei, Q. Deng, C. Yang, Q. Peng, H. Hou, Y. Li and K. Li, *Mater. Chem. Front.*, 2019, **3**, 2746-2750.
- (a) Q. Feng, Y. Li, L. Wang, C. Li, J. Wang, Y. Liu, K. Li and H. Hou, *Chem. Commun.*, 2016, **52**, 3123-3126; (b) Y. He, Y. Li, H. Su, Y. Si, Y. Liu, Q. Peng, J. He, H. Hou and K. Li, *Mater. Chem. Front.*, 2019, **3**, 50-56.
- (a) J. Zhang, Q. Liu, W. Wu, J. Peng, H. Zhang, F. Song, B. He, X. Wang, H. H. Y. Sung, M. Chen, B. S. Li, S. H. Liu, J. W. Y. Lam and B. Z. Tang, *ACS Nano*, 2019, **13**, 3618-3628; (b) Y. Li, Q. Peng, S. Li, Y. Cai, B. Zhang, K. Sun, J. Ma, C. Yang, H. Hou, H. Su and K. Li, *Sens. Actuators B Chem.*, 2019, **301**, 127139.
- Y. J. Kong, Z. P. Yan, S. Li, H. F. Su, K. Li, Y. X. Zheng and S. Q. Zang, *Angew. Chem. Int. Ed.*, 2020, DOI: 10.1002/ange.201915844.
- (a) H. M. Kim, Y. O. Lee, C. S. Lim, J. S. Kim and B. R. Cho, *The J. Org. Chem.*, 2008, **73**, 5127-5130; (b) C. Lavanya Devi, K. Yesudas, N. S. Makarov, V. Jayathirtha Rao, K. Bhanuprakash and J. W. Perry, *J. Mater. Chem. C*, 2015, **3**, 3730-3744; (c) Y. Shi, Z. Li, Y. Fang, J. Sun, M. Zhao and Y. Song, *Opt. Laser Technol.*, 2017, **90**, 18-21.